HHS Public Access

Author manuscript

Hyg Environ Health Adv. Author manuscript; available in PMC 2023 September 14.

Published in final edited form as:

Hyg Environ Health Adv. 2023 September ; 7: . doi:10.1016/j.heha.2023.100074.

Toxicity assessment of CeO_2 and CuO nanoparticles at the air-liquid interface using bioinspired condensational particle growth

Trevor B. Tilly[a,b], **Ryan X. Ward**[a], **Alyssa F. Morea**[a], **M. Tyler Nelson**[b], **Sarah E. Robinson**[c], **Arantzazu Eiguren-Fernandez**[d], **Gregory S. Lewis**[d], **John A. Lednicky**[c], **Tara Sabo-Attwood**[c], **Saber M. Hussain**[b], **Chang-Yu Wu**[a,*]

[a]Department of Environmental Engineering Sciences, Engineering School of Sustainable Infrastructure and Environment, University of Florida, Gainesville, FL, United States

[b]711th Human Performance Wing, Air Force Research Laboratory, Wright-Patterson AFB, Ohio, United States

[c]Department of Environmental & Global Health, College of Public Health and Health Professions, University of Florida, Gainesville, FL, United States

[d]Aerosol Dynamics Inc., Berkeley, CA, United States

Abstract

CeO_2 and CuO nanoparticles (NPs) are used as additives in petrodiesel to enhance engine performance leading to reduced diesel combustion emissions. Despite their benefits, the additive application poses human health concerns by releasing inhalable NPs into the ambient air. In this study, a bioinspired lung cell exposure system, Dosimetric Aerosol *in Vitro* Inhalation Device (DAVID), was employed for evaluating the toxicity of aerosolized CeO_2 and CuO NPs with a short duration of exposure (≤10 min vs. hours in other systems) and without exerting toxicity from non-NP factors. Human epithelial A549 lung cells were cultured and maintained within DAVID at the air-liquid interface (ALI), onto which aerosolized NPs were deposited, and experiments in submerged cells were used for comparison. Exposure of the cells to the CeO_2 NPs did not result in detectable IL-8 release, nor did it produce a significant reduction in cell viability based on lactate dehydrogenase (LDH) assay, with a marginal decrease (10%) at the dose of 388 μg/cm^2 (273 cm^2/cm^2). In contrast, exposure to CuO NPs resulted in a concentration dependent reduction in LDH release based on LDH leakage, with 38% reduction in viability at the highest dose of 52 μg/cm^2 (28.3 cm^2/cm^2). Cells exposed to CuO NPs resulted in a dose dependent cellular membrane toxicity and expressed IL-8 secretion at a global dose five times lower than cells exposed under submerged conditions. However, when comparing the ALI results at the local cellular dose of CuO NPs to the submerged results, the IL-8 secretion was similar. In this study, we demonstrated DAVID as a new exposure tool that helps evaluate aerosol toxicity in simulated lung environment. Our results also highlight the necessity in choosing the right assay endpoints for

*Corresponding author. cywu@essie.ufl.edu (C.-Y. Wu).

Supplementary materials

Supplementary material associated with this article can be found, in the online version, at doi:10.1016/j.heha.2023.100074.

the given exposure scenario, e.g., LDH for ALI and Deep Blue for submerged conditions for cell viability.

Keywords

Nanotoxicology; In vitro; Aerosol exposure; Deposition; Air-liquid interface

Introduction

There are numerous benefits for using engineered nanoparticles (NPs) as fuel-borne additives in petrodiesel, including the reduction of hazardous emissions, decreases in fuel consumption, extension of the performance life of diesel particulate filter through oxidation of soot, and increases in engine performance (Saxena et al., 2017; Chandrasekaran et al., 2016; Balamurugan et al., 2013; Setiabudi et al., 2004). In comparison to gasoline engine emissions, exhaust from petrodiesel combustion contains a higher mass concentration of particulate matter, which has been linked to morbidity and mortality in humans (Ristovski et al., 2012). Metal oxide NPs, such as cerium oxide (CeO_2) and copper oxide (CuO), have been applied in reducing hazardous emissions by lowering the carbon combustion temperature requirement and oxidizing the remaining hydrocarbons (Norhafana et al., 2020). However, the application of NPs as fuel additives also creates a human health concern by increasing their ambient environmental exposure (Snow et al., 2014; Cassee et al., 2011; Zhang et al., 2013).

CeO_2 NPs are commercially available as petrodiesel additives under multiple names: Envirox, Eolys, and Platinum Plus (a Pt and Ce based material) (Dale et al., 2017; Erdakos et al., 2014). As an example of human inhalation exposure, the ambient concentration of CeO_2 NPs was shown to increase in Newcastle and London, England by as much as fourfold after public transportation buses started using Envirox supplemented diesel fuels (Park et al., 2008). Although only a fraction of the buses used the supplemented fuel and the total ambient CeO_2 NP concentration was low at < 1 ng/m^3, it provides rationale to assess the toxicity of NPs with focus on inhalation (Cassee et al., 2011). Because there are a multitude of new NPs being developed and incorporated in consumer and industrial goods, it is infeasible to conduct toxicity screening in vivo using animals due to the required cost and experimental time necessary. Furthermore, there are physiological differences in the respiratory system of the humans and animals that complicate the toxicological relation to human health effects (Fröhlich and Salar-behzadi, 2014). While in vitro methods have limitations in studying the transport of materials and cell communications, they have advantages in evaluating the toxicity of NPs, such as incorporation of cells from the human respiratory tract, the relative low cost, and having less experimental time to make the toxicity assessment (Stewart et al., 2012). However, in vitro toxicity analysis of airborne NPs has not commonly been assessed in a manner that reflects the *in-situ* condition (aerosolized exposure).

In a conventional in vitro toxicity test, the NPs are dispersed in a liquid medium, i.e., submerged, where they passively interact with cells by sedimentation and diffusional

transport over the course of exposure. Although submerged in vitro methods are relatively simple to conduct and provide insight into the toxicity potential of NPs, interpretation of their results has its limitations. Firstly, homogeneous dispersion of NPs can be difficult to achieve and any heterogeneity will influence their dosimetry and subsequent toxicity to cell culture (Tilly et al., 2014). The differences in particokinetics in exposure medium between various types of particles makes the dosimetric consideration a necessity for toxicity assessment (Teeguarden et al., 2007); nevertheless, it is often neglected (DeLoid et al., 2017). Secondly, by transferring NPs from aerosol phase to liquid phase, their physical and chemical properties may be altered, which can include changes to agglomeration, surface functionality and dissolution of ions into the medium (Tilly et al., 2019; Tilly et al., 2020). These changes in the physicochemical properties of the NPs that occur through dispersion in liquid have been shown to alter their cellular response and toxicity outcome (Lichtveld et al., 2012). Thirdly, the interference of the NPs with toxicity assays during submerged cell exposure has been well reported, caused by the binding of NPs to the analyte biomolecule or by reaction with assay reagents to produce false results (Holder et al., 2012; Ong et al., 2014; Kroll et al., 2009; Kroll et al., 2012; Inman and Zhang, 2009). To overcome the limitations caused by conducting toxicity analysis of NPs in submerged cell cultures, as well as to better simulate the in vivo exposure scenario, methods to culture and expose cells at the air-liquid interface (ALI) have been developed and recently grown in popularity (Hussain et al., 2015).

Despite the numerous methodological and physiological benefits by conducting toxicity evaluation of NPs in ALI cell culture, the use of ALI system has been largely limited by the small number of NP delivery systems available. Moreover, during the exposure, NPs generally have a low deposition efficiency. Therefore, a large quantity of NPs has to be aerosolized to achieve the lowest observed adverse effect level (LOAEL) in short exposure times. For instance, the deposition of aerosol particles in the popular Vitrocell exposure chamber was shown to be less than 0.02% for 0.51 μm MMD (mass median diameter) particles and ~0.51% for 3.3 μm MMD particles (Oldham et al., 2019). Further, there was reported large variability in the deposited dose between replicate exposure wells and trials (Oldham et al., 2019); the variability makes it irrational to predict the delivered dose of NPs from the generalized deposition efficiency and then relate it to the biological outcome. The deposition in another commercial exposure system, Cultex, was also shown to have low efficiency with only 0.05% and 1.1% of Cu NPs deposited from two aerosols with geometric mean diameters of 80 and 180 nm, respectively (Elihn et al., 2015). Improvements in these systems as well as other flow-through aerosol exposure devices have been made through the addition of mechanisms to enhance NP deposition, such as electrostatics and thermophoresis.

The integration of electrostatic or thermophoretic mechanisms with existing aerosol exposure devices has been shown to enhance NP deposition, with studies reporting enhancements in deposition from 20% to almost an order of magnitude by inclusion of these techniques (Mülhopt et al., 2016; Broßell et al., 2013). However, deposition of NPs using these mechanisms is size-dependent (unipolar charging efficiency and thermophoretic efficiency is based on particle size) (Dixkens and Fissan, 2010). They still have low efficiency that ultimately results in a NP dose too low to produce a biological response

and that complicates their use for toxicity evaluation (Tilly et al., 2019). Further, the heating required for thermophoresis or the charging of the particles required by electrostatics has little relevance to how NPs are exposed in the human respiratory system, and the processes can alter the particle characteristics and consequently the toxicity outcome (Tilly et al., 2020).

Without deposition enhancement, the experimental exposure time needed to observe significant adverse effects is long, complicating the toxicity outcome and decreasing the convenience for in vitro cell culture in toxicity analysis. Furthermore, many exposure chambers were originally designed without humidity and temperature control for the aerosol and the lack of control resulted in cellular damage during exposure (Kooter et al., 2017). Auxiliary systems have been added to exposure chambers to heat and humidify the influent aerosol to a relative humidity (RH) >75% and temperature of 37 °C to prevent toxicity intrinsic to the system itself (Zavala et al., 2017). Consequently, altering the RH and temperature of the aerosol in these systems requires dilution with warm humid air in order to achieve temperature and RH conditions relevant to the human respiratory system and the dilution inherently lowers the particle concentration. Thereby, these conditions in existing ALI exposure systems make toxicity assessment of NPs sampled directly from the real-world environment unachievable in a reasonable timescale.

With its highly efficient particle deposition achieved by condensational particle growth (CPG), the Dosimetric Aerosol *in Vitro* Inhalation Device (DAVID) was designed to overcome the temperature and humidification limitations, to reduce the long exposure time required to achieve the LOAEL, and to increase the size range of particle deposition down to 10 nm. DAVID is a laminar flow water CPG system that preconditions the incoming aerosol to temperature and humidity comparable to human respiratory system, thereby reducing stress on lung cells during exposure. Airborne particles are efficiently deposited regardless of the original particle size, as the three-stage growth technology efficiently grows particles from all sizes to an asymptotic size in the micron size range based on the residence time and water vapor concentration (Hering et al., 2005). The collection and deposition efficiency of the CPG technology used in DAVID has been previously proven in the collection of aerosol particles containing viable virus, the same size scale as NPs, with 10–100 fold better collection efficiency than the industry standard of BioSampler® (Pan et al., 2016; Lednicky et al., 2016). More recently, DAVID was demonstrated to have highly efficient NP deposition for cell exposure, with negligible variation in dosing between replicate experiments and no stress to cells exposed to clean air (Tilly et al., 2019). Further, DAVID was demonstrated in the toxicity evaluation of freshly generated welding fume (Ward et al., 2020). Exposure in DAVID was bioinspired by the human respiratory system, where RH reaches supersaturation and inhaled particles initiate the condensation of water vapor to grow in physical size before being deposited throughout the respiratory tract (Longest and Xi, 2008). Further representation to human lung exposure by DAVID is achieved by particle deposition through jet nozzles, which results in focused spots. With resemblance to what occurs at bifurcations in the human lungs where concentrations exceed 100 times the average respiratory dose (Balásházy et al., 2003), the focused deposition offers an alternative to the uniform deposition toxicological model that is commonly used, though low clearance

mechanisms are an additional contributing factor to the vulnerability of these sites that should also be considered.

In this study, A549 cells cultured at ALI in DAVID were exposed to aerosolized CuO and CeO_2 NPs at 37 °C and 100% RH. The NPs were selected to demonstrate the utility of DAVID for physiologically relevant nanotoxicity assessment with a short exposure duration (≤ 10 min) and consistent deposition: CuO NPs have been shown to be toxic when exposed in submerged cell culture while CeO_2 NPs have low toxicity (Karlsson et al., 2008; Li et al., 2016). As the baseline for comparison to the ALI result, submerged toxicity assessment with the same NPs was conducted with two types of assays for cell viability and an immunosorbent assay for proinflammatory response. The toxicity of the NPs to the ALI cells was determined both across the global cell culture and at the local NP deposition spots, based on both mass and surface area doses.

Materials and methods

Nanomaterials

CuO and CeO_2 nanopowders were purchased from US Research Nanomaterials Inc. (Houston, TX, USA). Synthesized by flame spray pyrolysis, the NPs had manufacturer reported diameters of 40 nm for the CuO and 10 to 30 nm for the CeO_2. Bruauer-Emett-Teller (BET) surface area of the NPs was measured using a NOVAe Series BET (Quantachrome, Boynton Beach, FL, USA) to determine the surface area dose in the toxicity analysis. Before analysis, the nanopowder samples were vacuum degassed for 0.5 hour at 200 °C.

Cell culture

A549 cells (CCL-185, American Type Cell Collection, Manassas, VA, USA) were used. As previously described (Tilly et al., 2019), the cells were cultured in glutamine-free RPMI 1640 base medium supplemented with 10% fetal bovine serum (Heat Inactivated FBS, Gibco, Carlsbad, CA, USA), 100-fold dilution of penicillin-streptomycin (Pen: 100 U/mL, Strep: 100 μg/mL, Gibco), and 100-fold dilution of GlutaMAX Supplement (35,050,061, Gibco). The cells were cultured to confluence before being treated with 0.25% trypsin-EDTA (0.25%, phenol red, Gibco) for detachment from flask, counted by hemocytometer, and seeded on custom cell culture supports for ALI exposure. The 36 mm^2 custom cell culture supports were 3D printed with polylactic acid filament (1.75 mm white, MakeShaper, Sanford, NC, USA) and assembled to the polyester membrane with nontoxic sealant (737 RTV, Dow Corning, Midland, MI, USA) as described previously (Tilly et al., 2019). The only difference in the polyester membrane (Sabeu, Cape Coral, FL) was the tissue-culture treatment at the manufacturing facility. A stock cell suspension was prepared and 0.1 mL of the cells were pipetted onto the culture membranes at a concentration of 59,400 cells/mL to establish the cell monolayer (Tilly et al., 2019; Lenz et al., 2013; Blank et al., 2006). After 72 hr of culture, the medium was replaced, and the apical medium was removed in preparation for aerosol exposure. Cells without basal medium leakage to the apical side 24–48 hr at the ALI were used for the cytotoxicity assessment.

Toxicity assessment assays

Three assays were used to compare the cellular effects of the two NPs resulting from aerosol exposure and submerged toxicity methods. The viability of the cells was assessed by the Deep Blue (DB, BioLegend, San Diego, CA) and lactate dehydrogenase (LDH, BioLegend) assays. The DB assay measures the cellular metabolism through a change in the fluorescence of the resazurin reagent, which assesses cell viability in comparison to control cells (Rampersad, 2012). The LDH assay is complementary to the DB assay for cell viability assessment, but it differs by quantifying the LDH released from the extracellular space when the plasma membrane is damaged (Chan et al., 2013). The proinflammatory response was assessed by interleukin-8 enzyme-linked immunosorbent assay (IL-8 ELISA, ELISA Max Deluxe Human ELISA, BioLegend); 50 μL of the basal medium from the cells exposed at the ALI was analyzed in triplicate following protocols set by the manufacturer for analysis in a 96-well plate. The IL-8 cytokine has been demonstrated as a good inflammatory indicator for A549 cells exposed to NPs (Monteiller et al., 2007). The interference of the NPs with the three assays was determined without cells in the culture medium for 24 hr to mimic the same conditions as the incubation period of the cell exposures. For the DB assay, 100 μL of DB assay dye was added to the culture medium at 10:1 and added apically to the ALI cultures. After incubation for 10 min, the apical samples were transferred from the supported membranes into a 96-well plate for measurement by the automated plate reader (Synergy H1, BioTek, Winooski, VT). The LDH assay was conducted by removing the basal medium, transferring 50 μL in triplicate to 96-well plate wells, for the ALI exposures. Finally, the ALI cell cultures were inspected post exposure to the NPs using light microscopy with 10x objective and 10x ocular. All cell culture methods, assay information, and results can be found in the supplementary information [link to SI].

ALI cell exposure in DAVID

The design and materials used to assemble DAVID have been described previously for the sequential spot sampler (Eiguren Fernandez et al., 2014), with major differences being that DAVID has eight CPG tubes in parallel and a chamber to expose ALI cell cultures to nano-aerosols. The aerosol pathway in DAVID, including the conditioner, initiator, moderator, nozzles, and cell exposure chamber, was machined from aluminum and anodized. The water wick for the CPG process was rolled 0.45-μm pore size nylon filter media (Whatman 10,416,194, Cytiva, Marlborough, Massachusetts).

The original DAVID was shown to be highly efficient for NP deposition (Tilly et al., 2019); however, improvements to the upgraded version of DAVID were utilized here to overcome limitations previously observed. These changes included a water injection pump for controllable wick wetting during exposure to achieve vapor saturation for consistent CPG and the addition of a vapor moderator stage to control the volume of water depositing with the NPs on the cells during exposure in order to prevent cellular hyponatremia. With these additions, the CPG growth droplet diameter size increased, which required the jet nozzle diameter to be increased from 0.66 mm to 1 mm to prevent clogging. Likewise, the number of jets exposing each cell cultures decreased from four to three to retain the high impaction efficiency with the large jet diameter. Each cell culture was exposed to aerosols from one nozzle with three jets at a distance of 5 mm. Exposures resulted in three NP deposition spots

per cell culture, observed by light microscopy and measured using ImageJ to determine the deposition area (Schneider et al., 2012). The three NP deposition spots on the surface of the cell cultures were measured to have an average diameter of 1.63 mm, making the average concentration of NPs in the spots the local deposited dose. Whereas, the global dose was the NPs concentration averaged across the entire cell culture surface area. The temperatures in DAVID were set as: conditioner at 5 °C, initiator at 40 °C, moderator at 30 °C, nozzles at 37 °C, and sample at 37 °C. The effect of the new flow and temperature settings in DAVID was evaluated by exposing ALI cultured A549 cells to clean air. No significant differences were observed in the cell viability and IL-8 production from incubator controls. Aerosol deposition was completed within 10 min to minimize the stress from long exposure encountered in other aerosol exposure systems.

Aerosol generation and monitoring

The NPs were aerosolized from either a dry powder by an acoustic aerosol generator or a suspension using a nebulizer. A 6-jet Collison nebulizer (BGI Inc., Waltham, MA) was used to generate aerosols from NP suspensions in 95% ethanol (Decon Labs Inc., King of Prussia, PA) with suspension concentrations from 0.1 to 10 mg/mL. Aerosolization of the NPs by the acoustic powder generator followed a previous study (Tilly et al., 2020), only differing by the use of 35 and 70 Hz frequencies simultaneously for agitation and aerosolization of the nanopowders, respectively. Based on particle number concentration measured by the aerosol monitoring equipment, dose considerations from other studies, the ALI cell exposure time was four minutes for acoustic aerosolization to achieve NP dose range of 5.9 to 152 $\mu g/cm^2$ (1.10 to 28.3 cm^2/cm^2) and 31 to 388 $\mu g/cm^2$ (21.8 to 273 cm^2/cm^2) for CuO and CeO_2 exposures, respectively. For nebulizer exposure, 10 min was selected to achieve a dose range of 0.39 to 2.87 $\mu g/cm^2$ (0.07 to 0.53 cm^2/cm^2) for CuO NPs and one dose of CeO NPs at 9.72 $\mu g/cm^2$ (6.85 cm^2/cm^2).

A schematic for the aerosol generation, monitoring and exposure is shown in Fig. 1. Compressed air (breathing quality grade, Air Liquide, Radnor, PA) at 9 or 12 LPM regulated by a rotameter (FLDA3216ST, Omega Engineering, Norwalk, CT) was sent to either a Collison nebulizer or an acoustic aerosol generator, respectively. The resulting aerosol was diluted with 16 LPM compressed air (breathing quality) regulated by the same type of rotameter. The nebulizer operation differed from the acoustic aerosol generator, as the nebulizer was placed in an ultrasonic bath to prevent settling of the NPs from suspension during the exposure. The liquid droplets generated by the nebulizer were dried and diluted by the dilution air to produce dry aerosol particles in the nanoscale. Cells in DAVID were exposed to the aerosol at a flow rate of 4 LPM. The time-averaged particle size distribution of each aerosol condition was measured by an aerodynamic particle sizer at 5 LPM (APS Spectrometer 3321, TSI Inc., Shoreview, MN, USA) and a scanning mobility particle sizer (SMPS), which consisted of a condensation particle counter operating at 1 LPM (CPC model 3010, TSI Inc., Shoreview, MN, USA) and a differential mobility analyzer (DMA 3081, TSI Inc., Shoreview, MN, USA). Excess flow in the system was exhausted to high-efficiency particulate arresting (HEPA) filter before discharge.

Statistics

Although there were too few observations to determine normality, each exposure was completed in four cell culture wells and each full experiment was repeated in triplicate ($n = 3$). Figures have values presented as mean with error bars as the standard error of the mean, and in the text the mean is presented. Statistical significance of the toxicologic end points was determined by one-way analysis of variance (ANOVA) using Analysis ToolPak in Excel (Microsoft, Redmond, WA) with $\alpha = 0.05$.

Nanoparticle dosimetry calculation and mass to surface area dose conversion

The mass dose for the ALI exposure was measured using inductively coupled plasma mass spectrometry (ICP-MS). The cell cultures attached to the membranes were digested in concentrated nitric acid for 24 hr and then diluted to 10 mL for analysis by ICP-MS (Agilent 7900 ICP/MS, Santa Clara, CA). The particle size and concentration measured by the APS/SMPS was also used to estimate the delivered dose of NPs to the cell cultures (global dose or local dose). The estimated mass dose in μg/cm^2 was calculated according to Eq. (1):

$$Mass\ Dose(ALI) = \frac{NQ\rho t}{A} \cdot \frac{\pi}{6} d_m^3 \cdot 10^{-12} \quad (1)$$

where ρ is the apparent density of the NPs characterized by the manufacturer (CuO: 0.55 g/cm^3, CeO_2 :0.95 g/cm^3), N is the aerosol particle number concentration (#/cm^3), Q is the volumetric flow rate of each exposure nozzle (LPM), t is the exposure time (min), A is the surface area of the cell culture membrane (36 mm^2) for global dose or surface area of the three deposition spots (6.26 mm^2) for the local dose, d_m (nm) is the diameter of average mass determined from the count median diameter and geometric standard deviation of the aerosol (Hinds, 1999), and 10^{-12} is a unit conversion when using the units listed above. The ALI surface area dose (cm^2/cm^2) was calculated as the product of the mass dose and the BET surface area of the NPs.

The mass dose of NPs to cells in the submerged cell exposure in μg/cm^2 was determined by Eqn. (2) following previously used methods (Deloid et al., 2014; Cohen et al., 2014):

$$Mass\ Dose(submerged) = \frac{cV}{A} \cdot F_D \quad (2)$$

where c is the administered NP mass concentration (μg/mL), V is the administered volume (0.1 mL), A is the surface area of the cell culture well (0.32 cm^2), and F_D is the deposition fraction of the NPs from a suspension during the 24-hr exposure based on literature (95% and 65% for CuO and CeO_2 NPs, respectively) (Deloid et al., 2014). The surface area dose of the submerged exposure was converted from the mass dose by the incorporation of the BET surface area of the NPs into this framework.

Results and discussion

ALI exposure and nanotoxicity evaluation

The size distributions of the CeO_2 and CuO NP aerosols produced by the acoustic generator and the nebulizer measured by the SMPS and the APS are shown in Fig. 2. The majority of the NP mass aerosolized by the acoustic generator was on the microscale while the aerosol generated by the nebulizer was on the nanoscale. The count median diameters of the CeO_2 aerosols generated by the nebulizer and acoustic disperser were 47.8 nm and 2.84 μm, respectively. At the highest suspension concentration of the CuO NPs, nebulization produced a bimodal distribution with a major peak at 25.9 nm and a second peak at 181 nm, whereas the acoustically generated aerosol had a median size of 2.46 μm. The 181 nm peak for the CuO had greatest prominence at the higher nebulizer solution concentration of 10 mg/mL, but this mode disappeared as suspension concentration decreased and approached 0.1 mg/mL, the lowest concentration used for IL-8 induction. The bimodal particle size distribution for CuO NP aerosols generated by a Collison nebulizer has been reported before for a 1 mg/mL particle suspension (Kim et al., 2013). Generating aerosols containing primary sized NPs when producing highly concentrated NP aerosols is a challenge for nebulization, as NPs under such conditions naturally agglomerate (Jaworek, 2007). Spark generated CuO NP aerosols with a median diameter of 9.2 nm have been achieved (Jing et al., 2015); however, to aerosolize NPs as primary particles from a nebulizer would require a very dilute concentration of NPs in the solution (May 1973), thus requiring long exposure (on the order of days) to achieve a delivered dose to cells necessary to elicit a response.

There were also particles generated on the nanoscale by the acoustic disperser measured by SMPS, shown in Figure S1; however, their contribution to the total deposited mass calculated by Eq. (1) to the cells was only 2% and 0.2% for the CuO and CeO_2 NPs, respectively. Therefore, the larger size mode of the aerosol measured by the APS represented the agglomerated NPs and accounted for the majority of the mass deposited during exposure. The two highest delivered mass doses of the CeO_2 and CuO NPs to the ALI cell cultures in the exposure trials were from the acoustic aerosol generation, and the lower doses were from the nebulizer.

The velocity used in DAVID is required for efficient impaction; if lowered, there would be high particle penetration. This makes the velocity requirement in DAVID impacting the cells higher than that in the human respiratory system, however, it is much lower than previous impaction cell exposure studies. For example, the effect of diesel exhaust exposure on lungs was assessed by inertial impaction, and required an exposure velocity of 45.5 m/s (Cooney and Hickey, 2011). Since they did not have CPG, the aerosolized particles will have high penetration at low flow rates, which has a disadvantage as the velocity required for particle deposition will also cause notable cell death. By adding CPG before the impactor, the viability of the cells was improved during exposure by reducing the jet velocity required for efficient deposition of particles on cells to 6 m/s (Tilly et al., 2019). The change in number (4 to 3) and diameter (0.66 to 1 mm) of the jet nozzles decreased the impaction velocity from 6.08 m/s to 3.54 m/s in the upgraded DAVID used in this study.

The CPG mechanism utilized by DAVID grew all particles in the generated aerosols to a uniform droplet size shown by the dotted curve in Fig. 2, which had a median of 7.77 μm for both types of NPs. The updated version of DAVID used in this study, with more effective water vapor control, produced a final median droplet size that was almost a micron greater than the original DAVID model (6.93 μm) (Tilly et al., 2019). The larger growth sizes of the NPs indicate that a high efficiency in particle deposition would still be achieved at the same operational flow rates used in the original DAVID, since the droplets possessed more inertia through greater water vapor condensation. The deposition of the NPs on the ALI cell cultures is based on the arrangement of the jet nozzles in DAVID. In this study, each cell culture was exposed to aerosol *via* three jets, which resulted in three focused spots on each ALI cell culture. This result is different from most exposure systems that attempt even deposition across the cell surface. The focused delivery of the NPs on the cell culture provides an important challenge in toxicity analysis, as biological assays are typically designed for global rather than local cellular response; as a result, certain assays provide more insight than others (Ward et al., 2020). Nevertheless, the spot pattern may have relevance to the in vivo inhaled NP toxicity scenario, where adverse health effects associated with inhaled NPs have been attributed to a small fraction of epithelial cells lining the respiratory system receiving dosages of particles hundreds of times greater than the global dose (Balásházy et al., 2003).

Though the NPs deposition in DAVID occurred in local spots, there were also NPs observed away from the deposition spot in nearby cells. Representative light microscopy images of the unexposed ALI cell culture control and ALI cells exposed to CuO and CeO_2 NPs are shown in Fig. 3. A confluent monolayer of the cells with anomalous morphology can be observed in the control cells and those exposed to the CeO_2 NPs, Fig. 3A and 3B, respectively. In contrast, the cells exposed to the CuO NPs, shown in Fig. 3C, began to exhibit inerratic spheroidal morphology indicative of cell stress and death (Wu et al., 2018). Interestingly, particles were also observed within cells that were near but outside the three focused deposition spots and featured inerratic spheroidal cellular morphology that is typically associated with cellular stress from exposure to biologic stressors (Ren et al., 2015).

After characterizing the aerosol and performing dosimetry analysis, the cell viability of the A549 cells exposed to NPs at the ALI was related to the global delivered mass and surface area doses across the membranes, shown in Figs. 4A–B. The surface areas of the CeO_2 and CuO NPs measured by BET were 70.5 m^2/g and 18.6 m^2/g, respectively. The surface area of the deposition spots measured in ImageJ was used to compare the cellular response at the local dose to the global dose calculated over the total surface area of the cell cultures. The diameter of each of the three deposition spots was 1.63 mm; therefore, the surface area of the combined three circular deposition spots on each cell culture was 6.26 mm^2. With the cell culture membranes having an area of 36 mm^2 making them 5.75 times greater in area than the deposition spots, and the NP deposition focused on 17.4% of the cell culture surface.

Considering the losses in the aerosol generation and transport to DAVID, the estimated dose was in relative agreement with the measured dose determined by ICP-MS for the

CeO_2 aerosol (all doses within 30%) and the highest dose within 5%. For the CuO aerosol exposure, the estimated and measured doses of the highest and third highest exposures had percent difference less than 15%, and the second highest dose estimation of the CuO NPs was within 31% difference from the measured dose. The estimated delivered doses of CuO and CeO_2 NPs were below the measured dose in the majority of exposures, except the middle CeO_2 exposure concentration. The differences in estimated and measured delivered dose were caused by the combination of assumptions made for the particle concentration measurement in Eq. (1) for size and particle number concentration due to the aerosol containing agglomerated NPs. Despite these assumptions, the dosing correlation was sufficient for estimating the exposure concentrations and times necessary to achieve lower delivered doses for the IL-8 analysis before completion of ICP-MS.

For the cell viability analysis, the DB assay reached saturation in under 10 min making the exposed and unexposed cell exposures indistinguishable. Similar to observations in previous studies (Ward et al., 2020), the poor performance of the DB assay was likely a result of the localized deposition of NPs on the cells in DAVID, which left the majority of the cells unexposed, thus masking/diluting any change in overall cell viability due to metabolic activity in proliferated cells. In contrast, the exposure of cells at the ALI overcame limitations in the use of the LDH assay for submerged nontoxicity testing, which has been shown to have NP interference with the LDH molecule (Ong et al., 2014; Kroll et al., 2009; Stone et al., 2009; Han et al., 2011). Unlike exposures in submerged cell culture where NPs are mixed with culture media, NPs are deposited apically to the cell surface in ALI exposures, thereby preventing NP contamination of the medium used for the toxicity analysis. Thus, only the LDH assay result is presented for the ALI, Figs. 4A–B. Cells exposed to CeO_2 remained viable at all exposure concentrations; with 90% viability at a delivered dose of 388 $\mu g/cm^2$ (273 cm^2/cm^2). This dose is considered a high exposure concentration, especially if arising from an ambient source (Wu and Biswas, 2005). The results imply that CeO_2 NPs have low toxicity, as they did not reduce cell viability through LDH release. In comparison, the CuO NP exposure at the ALI decreased LDH cell viability with statistical significance at the three highest doses, with the greatest decrease in cell viability of 62% at a dose of 152 $\mu g/cm^2$ (28.3 cm^2/cm^2). It should also be noted that such high doses were attained in DAVID in 10 or less minutes of NP exposure, thus minimizing the impact on cells resulting from long exposure time experienced in other aerosol exposure systems.

The efficient NP deposition in DAVID prioritized the selection of relevant dose ranges in order to effectively relate in vitro and in vivo toxicity data. Thus, the relatively high dose range in Figs. 4A–B was chosen to observe a modest cell viability response, while the aerosol concentration and exposure time were adjusted to achieve lower delivered NP doses to increase the biological relevance in determining the IL-8 response. IL-8 induction (% fold change from IL-8 baseline exposure control) of the A549 cells exposed to the NPs at the ALI based on mass and surface area doses is shown in Fig. 4C and 4D, respectively. For unexposed ALI cell cultures, there was an IL-8 baseline of 119 pg/mL, and those exposed to clean air in DAVID had an average of 137 pg/mL. Since CeO_2 NPs did not decrease viability at even the highest concentrations, there was only one dose used for IL-8 induction, which was almost 13-fold mass concentration or 3.5-fold surface area concentration greater

than the largest CuO NP dose. In comparison to the viability, a much lower mass dose of CuO NPs stimulated a statistically significant IL-8 response; the two highest exposure doses of 1.48 μg/cm^2 (0.22 cm^2/cm^2) and 2.87 μg/cm^2 (0.53 cm^2/cm^2) produced a 3.4-fold and 8.5-fold change, respectively. The CeO_2 NP exposure at 9.72 μg/cm^2 (6.85 cm^2/cm^2) resulted in lower IL-8 secretion than the control with a 0.71-fold change.

Endpoint toxicity analysis of the cells exposed to the NPs under focused deposition spots differs from the global response. Since the lysis of the entire cell culture is the positive control for the LDH assay, the actual cell viability at the local deposition spots was lower than the 61.7% viability shown at the highest CuO dose of 152 μg/cm^2 (28.3 cm^2/cm^2), due to the greater dose at the deposition spots than the global dose reported. The IL-8 response could be related to the local delivered dose, as the IL-8 cytokine was secreted into the basal medium proportional to the exposed cells. Thus, IL-8 is not only a sensitive dose-dependent marker for evaluating NP toxicity at the ALI, but also one that can be used in an uneven exposure and related to the local deposited dose. However, relating the surface area of the entire culture and at the three deposition spots may not be perfect, as cells transport materials through endo- and exocytosis, which can transport the NPs away from where they were deposited (Paur et al., 2011). Further transport of NPs across cell cultures can be facilitated by ciliated cells, which can be found in differentiated primary ALI cell cultures (Stewart et al., 2012). Alternatively, the NPs can diffuse in cellularly produced mucin that is produced by A549 cells when cultured at the ALI (Wu et al., 2018). Since non-ciliated A549 cells were utilized in this study, the CuO NPs observed in cells located outside of the focused deposition spots, Fig. 3C, were likely due to cellular endo/exocytosis and transport in mucin.

Submerged vs. ALI in vitro exposure

In comparing the cell viability of the submerged and ALI NP exposures, the response of the cells exposed to CuO NPs occurred at a concentration over 50-times lower in submerged cell culture than for cells grown at the ALI (Figure S2 for submerged vs Fig. 4 for ALI). The submerged cell viability measured by the DB assay was dose dependent for the CuO NP exposures; however, we did not have a LDH result due to particle interference with the LDH assay probe. The methodological differences of the DB and LDH assays can contribute to the 50-fold difference in submerged and ALI exposure toxicity. The difference may also be attributed to the potency of CuO NPs to submerged cell culture at low administered doses, which can be accredited to their relatively fast sedimentation rate (>95% in 24 hour) (Deloid et al., 2014) and their ability to form ions (Karlsson et al., 2008), leading to their use as a positive control in submerged toxicity studies (Tilly et al., 2014). The localized deposition of NPs in DAVID was also a contributor to the differences between the DB toxicity outcomes at the ALI and in submerged cell culture, as most cells exposed at the ALI were located outside the exposure jet and remained active to metabolize the DB dye and mask the reduction of cell viability caused by NP exposure. However, others have also reported greater toxicologic response of submerged cells exposed to lower NP concentration than at the ALI, which may be due to greater toxicologic resiliency of the ALI cell culture over submerged cells during exposure (Panas et al., 2014).

Paralleling the viability findings, CeO_2 neither caused IL-8 secretion in the submerged or the ALI cell cultures, shown in Fig. 5. The CuO NPs at the highest dose did stimulate a significant IL-8 response with up to 3.5-fold change increase in submerged cells and 8.5-fold increase when exposed at the ALI. Interestingly, the greatest IL-8 secretion at the ALI after exposure occurred at a global dose of 2.87 μg/cm^2 (0.53 cm^2/cm^2), than the submerged at 7.42 μg/cm^2 (1.38 cm^2/cm^2). The same 3.5-fold IL-8 change for the ALI exposure occurred at a global dose of 1.18 μg/cm^2 (0.22 cm^2/cm^2), which was over five times lower than the submerged delivered dose. The difference in dose response of the two systems was resolved by relating the IL-8 change to the local dose of NPs deposited on the ALI cells, shown in Fig. 5. With the total culture area being 5.75 times larger than the deposition spot, the local delivered dose was 8.5 μg/cm^2 (1.58 cm^2/cm^2) to cause the 3.5-fold IL-8 change at the ALI. As shown in Fig. 5, the dose dependent IL-8 responses for the ALI and submerged cell exposures were similar when the NPs dose at the ALI was determined locally. Similarity in response for the A549 cells exposed under submerged and ALI conditions was not unexpected since A549 is an immortalized cell line, which limits their ability to differentiate when cultured at the ALI (Bérubé et al., 2009). Additionally, the comparable result for A549 cells exposed to NPs at the ALI and submerged may be explained by multiple genes for metal homeostasis, oxidative stress, apoptotic factors and DNA damage having similar expression in both exposure scenarios (Hufnagel et al., 2020). The A549 cells were selected in this study due to their popular use in ALI NP exposure studies, thereby aiding in comparison to previous work and accelerating the development of the exposure protocols in DAVID. The use of a differentiating in vitro model like small airway epithelial cells (SAECs) should be investigated in future studies to better understand the toxicologic differences of NPs exposed under submerged and ALI conditions.

The localized deposition in DAVID may better emulate the in vivo deposition of NPs than a uniform dose, as it has been shown to occur at bifurcations in the lung (Balásházy et al., 2003). However, many assays measure the global cellular response, and localized deposition can complicate the toxicity result by leaving some cells unexposed. Aerosol exposure chambers are still being improved, which makes homogenous deposition the key to understand the global cellular response. On the contrary, the well-defined NP deposition spot on the cell culture achieved in DAVID afforded the ability to relate the local delivered dose to the cellular inflammatory response. There is the potential to further test the effects of localized and evenly distributed NPs deposition on ALI cell culture by rotating the cell cultures at low speeds (6 RPM) under the jet nozzles during exposure (Fernandez et al., 2020).

The toxicity response of cell cultures exposed to diesel exhaust particles, carbon nanotubes, and ZnO NPs at the ALI has been shown to be more sensitive in comparison to submerged culture (Lichtveld et al., 2012; Lenz et al., 2013; Holder et al., 2008; Fröhlich et al., 2012; Raemy et al., 2012; Hilton et al., 2019). However, the opposite result was shown in the exposure of silica and silver NPs, where the same toxicity response occurred at lower dosages for cells exposed submerged than cells at the ALI (Panas et al., 2014; Herzog et al., 2014). The difference in sensitivity at the ALI and in submerged culture may be explained by differences in particle interactions in solution and in an aerosol and subsequent cell exposure in a chamber. While choice of cell culture could also affect the toxicity

outcome, all of the mentioned studies used immortal cell lines in their cell exposures with all but two of the studies using the A549 cell line or a co-culture with the A549 cell line. Thus, the differences in toxicity observed in these studies was potentially due to the selection of toxicity endpoints and relation to the ALI and submerged exposure cultures with non-standard reported dosimetry, which consequently complicated the comparison of NP dose to the observed biologic responses in ALI exposure studies.

Comparing nanoaerosol exposures

The toxicity assessment of CeO_2 NPs at the ALI in the literature provides examples of conflicting toxicologic results. One study, using a Cultex exposure chamber without deposition enhancement, found only 45% of A549 cells remained viable after exposure to CeO_2 NPs at a delivered dose of 100 μg/cm^2, as assessed by the water soluble tetrazolium assay (Rach et al., 2014). However, the delivered dose was not validated for the CeO_2 NPs but predicted based on 10–35% deposition efficiency (Rach et al., 2014), which was substantially greater than the 2% deposition efficiency determined by others with the same system (Elihn et al., 2015). Considering the uncertainty in the actual delivered dose, toxicity effects in that study might have been caused by the exposure method alone, as in that study two other aerosols of lactose monohydrate and P25 TiO_2, known to have low toxicity, also caused significant reduction in cell viability, with the TiO_2 NPs decreasing cell viability by an even greater extent than the CeO_2 NPs (Rach et al., 2014). Indeed, there was no verification if the aerosol exposure chambers themselves in that study had operationally induced cellular effects (Rach et al., 2014). In contrast, similar to what was observed in this study, CeO_2 NPs were shown to be readily taken up by the cells without causing any apparent dose-related toxicity at concentrations > 30 μg/cm^2 (Raemy et al., 2011; Kooter et al., 2016). More recently, researchers evaluating the performance of three ALI cell culture models for inhalation toxicity showed that CeO_2 NPs were nontoxic in all of the cell models, and a delivered dose of NPs at over 890 μg/cm^2 was required to elicit a cytotoxic response (Leibrock et al., 2019). The lack of toxicological and inflammatory response within physiological exposure concentration ranges justified the use of the higher dosing range in this study.

Results for toxicity of CuO NPs at the ALI are generally less conflicting. CuO NPs can be generalized as relatively toxic, especially in comparison to CeO_2. One study demonstrated a custom designed chamber with electrostatic precipitation exposing A549 cells to CuO NPs produced a similar LDH response to our findings with > 80% loss in viability at the maximum delivered dose (Tilly et al., 2020). Another study showed similar results, using the Vitrocell 6-well module to expose A549 and normal human bronchial epithelial cells to CuO NPs that exhibited a dose-dependent decrease in viability, LDH release, and increase in IL-8 secretion; between them, the A549 cells showed a more pronounced cell viability and LDH response, but lower IL-8 secretion (Jing et al., 2015). The exposure times were two and four hours to deposit 0.074 and 0.15 μg/cm^2, respectively, based on a predicted deposition efficiency of 50% (Jing et al., 2015). On the contrary, another group using the Vitrocell 3-well module did not observe toxicity after exposing cells to CuO NPs for one hour. However, the authors did not determine the deposited dose (Kooter et al., 2017); only the exposure concentration was given, and the NP deposition efficiency was determined by

scanning electron microscopy to be 3.3%. This conflicts with the more recently reported spatial variability across the cell culture surface and deposition efficiency of less than 0.02% for submicron particles in the Vitrocell exposure module (Oldham et al., 2019).

Difficulty in achieving consistent deposition in exposure systems is likely the reason for the complicated toxicological outcomes and may be a reason for their slow adoption over submerged cell culture exposure methods. With proper NP suspension preparation, homogeneous exposure across the cell culture surface is intrinsic to submerged cell exposure, as sedimentation and diffusion of the particles is predictable and controllable (Cohen et al., 2014). However, the limitations of submerged cell exposure discussed earlier to assess novel particle exposures mean that submerged exposure cannot provide a platform for direct cell exposure to aerosol-phase particles. All the above together warrant development of consistent, controlled, efficient, and short-duration deposition of NPs on ALI cell cultures in direct aerosol exposure systems without system-associated toxicity.

Conclusions

While new methods for exposing ALI cell cultures have shown promise in meeting the toxicity assessment demands of emerging NP exposures previously limited by traditional submerged methods, there are still obstacles to overcome in cell exposure at the ALI caused by the lack of standardization in characterizing the dosimetry between instruments and experiments. DAVID, which mimics the human respiratory system by using CPG to efficiently deposit NPs onto the ALI cell cultures without exerting system-associated toxicity, was demonstrated for nanoaerosol exposure in the lab. Unlike other aerosol exposure chambers, the efficient and gentle deposition of airborne NPs onto the ALI cells in DAVID provides a new exposure tool with reproducible results, which overcomes the variations in relating the biological effect to the delivered dose observed in some other aerosol exposure systems. In this study, DAVID was demonstrated to deliver a NP dose to ALI cells to observe cytotoxicity in very short exposure periods (≤10 min). Cells exposed to CeO_2 NPs, both submerged and ALI, did not have IL-8 induction and showed modest decreases in cell viability only at the greatest dosing levels. The CuO NPs, as hypothesized, decreased cell viability and produced IL-8 secretion when exposed in both types of cell culture. For the IL-8 response, the ALI and submerged exposed A549 cells had a similar dose response when the ALI delivered dose was determined locally and not averaged across the entire cell culture surface. The different cell viability responses for cells exposed to CuO at the ALI and the submerged demonstrate the importance of choosing the right assay endpoints for the given exposure system. Future studies should investigate how toxicologic outcome is affected by focused and evenly distributed NP deposition on ALI cells.

Supplementary Material

Refer to Web version on PubMed Central for supplementary material.

Acknowledgements

Authors would like to thank the UF College of Engineering Institute for Networked Autonomous Systems (INAS) Fellowship, UF University Scholars Program, National Institutes of Health Grant numbers: R21AI123933

and 1R43ES030649, and the Science Mathematics and Research for Transformation (SMART) Program with sponsorship by the 711th Human Performance Wing of the U.S. Air Force Research Laboratory, for the support of this work. Additionally, the authors would like to acknowledge the undergraduate researchers: Katie Rankin, Meg Simms, Mayuko Mizutani, Ricardo Aleman, Lauren Judah, Fiona Tennyson, Gan Huang, Kiran Mital, and Jina Yang, who aided in preparation and testing of the DAVID exposure unit.

Declaration of Competing Interest

The authors declare that "Toxicity Assessment of CeO_2 and CuO Nanoparticles at the Air-Liquid Interface Using Bioinspired Condensational Particle Growth" has not been published previously, and is not under consideration for publication elsewhere. The publication is approved by all authors and tacitly the responsible authorities where the work was carried out, and that, if accepted, it will not be published elsewhere in the same form, in English or in any other language, including electronically without the written consent of the copyright-holder.

The manuscript was approved for publication in Hygiene and Environmental Health Advances by the US Air Force with clearance by the 88 ABW on 27 August under case number 88ABW-2020–2701.

The funding for the research was declared in the acknowledgements section of the manuscript, and no third-party or outside work support was associated with this project other than that mentioned by government agencies.

The authors would like to disclose that US2020/0407675A1 patent application was published on Dec. 31, 2020 for the DAVID exposure system described in the manuscript: EFFICIENT DEPOSITION OF NANO - SIZED PARTICLES ONTO CELLS AT AN AIR LIQUID INTERFACE.

With these declarations of interest, we are happy to submit for publication in Hygiene and Environmental Health Advances.

Trevor Tilly, PhD

References

Bérubé K, Aufderheide M, Breheny D, Clothier R, Combes R, Forbes B, Gaça M, Gray A, Hall I, Kelly M, Lethem M, Liebsch M, Merolla L, Morin J, Seagrave J, a Swartz M, D TT, M. Umachandran, 2009. In Vitro models of inhalation toxicity and disease. Alta 37, 89–141.

Balásházy I, Hofmann W, Heistracher T, 2003. Local particle deposition patterns may play a key role in the development of lung cancer. J. Appl. Physiol 94, 1719–1725. 10.1152/japplphysiol.00527.2002. [PubMed: 12533493]

Balamurugan K, Tamilvanan A, Anbarasu M, Mohamed SA, Srihari S, 2013. Nano-copper additive for reducing NOx emission in soya bean biodiesel-fuelled CI engine. J. Biofuels 4, 1–8.

Blank F, Rothen-rutishauser BM, Schurch S, Gehr P, 2006. An optimized in vitro model of the respiratory tract wall to study particle cell interactions. J. Aerosol Med 19, 392–405. [PubMed: 17034314]

Broßell D, Tröller S, Dziurowitz N, Plitzko S, Linsel G, Asbach C, Azong-Wara N, Fissan H, Schmidt-Ott A, 2013. A thermal precipitator for the deposition of airborne nanoparticles onto living cells-Rationale and development. J. Aerosol Sci 63, 75–86. 10.1016/j.jaerosci.2013.04.012.

Cassee FR, Van Balen EC, Singh C, Green D, Muijser H, Weinstein J, Dreher K, 2011. Exposure, health and ecological effects review of engineered nanoscale cerium and cerium oxide associated with its use as a fuel additive. Crit. Rev. Toxicol 41, 213–229. 10.3109/10408444.2010.529105. [PubMed: 21244219]

Chan FK-M, Rosa K, De Rosa MJ, 2013. Detection of necrosis by release of lactate dehydrogenase (LDH) activity. Methods Mol. Biol 979, 65–70. 10.1007/978-1-62703-290-2. [PubMed: 23397389]

Chandrasekaran V, Arthanarisamy M, Nachiappan P, 2016. The role of nano additives for biodiesel and diesel blended transportation fuels. Transp. Res. Part D 46, 145–156. 10.1016/j.trd.2016.03.015.

Cohen JM, Teeguarden JG, Demokritou P, 2014. An integrated approach for the in vitro dosimetry of engineered nanomaterials. Part. Fibre Toxicol 11, 1–12. [PubMed: 24382024]

Cooney DJ, Hickey AJ, 2011. Cellular response to the deposition of diesel exhaust particle aerosols onto human lung cells grown at the air-liquid interface by inertial impaction. Toxicol. Vitr 25, 1953–1965. 10.1016/j.tiv.2011.06.019.

Dale JG, Cox SS, Vance ME, Marr LC, Hochella MF, 2017. Transformation of cerium oxide nanoparticles from a diesel fuel additive during combustion in a diesel engine. Environ. Sci. Technol 51, 1973–1980. 10.1021/acs.est.6b03173. [PubMed: 28112928]

Deloid G, Cohen JM, Darrah T, Derk R, Rojanasakul L, Pyrgiotakis G, Wohlleben W, Demokritou P, 2014. Estimating the effective density of engineered nanomaterials for in vitro dosimetry. Nat. Commun 5, 1–10. 10.1038/ncomms4514.

DeLoid GM, Cohen JM, Pyrgiotakis G, Demokritou P, 2017. Preparation, characterization, and in vitro dosimetry of dispersed, engineered nanomaterials. Nat. Protoc 12, 355–371. 10.1038/nprot.2016.172. [PubMed: 28102836]

Dixkens J, Fissan H, Development of an electrostatic precipitator for off-line particle analysis development of an electrostatic precipitator for off-line particle analysis, 6826 (2010). 10.1080/027868299304480.

Eiguren Fernandez A, Lewis GS, Hering SV, 2014. Design and laboratory evaluation of a sequential spot sampler for time-resolved measurement of airborne particle composition. Aerosol Sci. Technol 48, 655–663. 10.1080/02786826.2014.911409. [PubMed: 25045199]

Elihn K, Cronholm P, Karlsson H, Midlander K, Wallinder IO, Moller L, 2015. Cellular dose of partly soluble cu particle aerosols at the air-liquid interface using an in vitro lung cell exposure system. J. Aerosol Med. Pulm. Drug Deliv 26, 84–93. 10.1089/jamp.2012.0972.

Erdakos GB, Bhave PV, Pouliot GA, Simon H, Mathur R, 2014. Predicting the effects of nanoscale cerium additives in diesel fuel on regional-scale air quality. Environ. Sci. Technol 48, 12775–12782. 10.1021/es504050g. [PubMed: 25271762]

Fernandez AE, Lewis GS, Spielman SR, Wu C-Y, Tilly TB, Efficient deposition of Nano - sized particles onto cells at an air liquid interface, US 2020/0407675 A1, 2020.

Fröhlich E, Salar-behzadi S, 2014. Toxicological assessment of inhaled nanoparticles: role of in Vivo, ex Vivo, in Vitro, and in silico studies. Int. J. Mol. Sci 4795–4822. 10.3390/ijms15034795. [PubMed: 24646916]

Fröhlich E, Bonstingl G, Höfler A, Meindl C, Leitinger G, Pieber T, Roblegg E, 2012. Comparison of two in vitro systems to assess cellular effects of nanoparticles-containing aerosols. Toxicol. Vitr 27, 409–417. 10.1016/j.tiv.2012.08.008.

Han X, Gelein R, Corson N, Wade-Mercer P, Jiang J, Biswas P, Finkelstein JN, Elder A, Oberdörster G, 2011. Validation of an LDH assay for assessing nanoparticle toxicity. Toxicology 287, 99–104. 10.1016/j.tox.2011.06.011. [PubMed: 21722700]

Hering SV, Stolzenburg MR, Quant FR, O'Berreit DR, Keady PB, 2005. A laminar-flow, water-based condensation particle counter (WCPC). Aerosol Sci. Technol 39, 659–672. 10.1080/02786820500182123.

Herzog F, Loza K, Balog S, Clift MJD, Epple M, Gehr P, Petri-Fink A, Rothen-Rutishauser B, 2014. Mimicking exposures to acute and lifetime concentrations of inhaled silver nanoparticles by two different in vitro approaches. Beilstein J. Nanotechnol 5, 1357–1370. 10.3762/bjnano.5.149. [PubMed: 25247119]

Hilton G, Barosova H, Petri-Fink A, Rothen-Rutishauser B, Bereman M, 2019. Leveraging proteomics to compare submerged versus air-liquid interface carbon nanotube exposure to a 3D lung cell model. Toxicol. Vitr 54, 58–66. 10.1016/j.tiv.2018.09.010.

Hinds WC, 1999. Aerosol Technology: Properties, Behavior, and Measurement of Airborne Particles, 2nd ed. John Wiley & Sons Inc.

Holder AL, Lucas D, Goth-goldstein R, Koshland CP, 2008. Cellular response to diesel exhaust particles strongly depends on the exposure method. Toxicol. Sci 103, 108–115. 10.1093/toxsci/kfn014. [PubMed: 18227103]

Holder AL, Goth-goldstein R, Lucas D, Koshland CP, 2012. Particle-induced artifacts in the MTT and LDH viability assays. Chem. Res. Toxicol 25, 1885–1892. 10.1021/tx3001708. [PubMed: 22799765]

Hufnagel M, Schoch S, Wall J, Strauch BM, Hartwig A, 2020. Toxicity and gene expression profiling of copper- And titanium-based nanoparticles using air-liquid interface exposure. Chem. Res. Toxicol 33, 1237–1249. 10.1021/acs.chemrestox.9b00489. [PubMed: 32285662]

Hussain SM, Warheit DB, Ng SP, Comfort KK, Grabinski CM, Braydich-stolle LK, 2015. At the crossroads of Nanotoxicology in vitro: past achievements and current challenges. Toxicol. Sci 147, 5–16. 10.1093/toxsci/kfv106. [PubMed: 26310852]

Inman AO, Zhang LW, 2009. Limitations and relative utility of screening assays to assess engineered nanoparticle toxicity in a human cell line. Toxicol. Appl. Pharmacol 234, 222–235. 10.1016/j.taap.2008.09.030. [PubMed: 18983864]

Jaworek A, 2007. Micro- and nanoparticle production by electrospraying. Powder Technol 176, 18–35. 10.1016/j.powtec.2007.01.035.

Jing X, Park JH, Peters TM, Thorne PS, 2015. Toxicity of copper oxide nanoparticles in lung epithelial cells exposed at the air-liquid interface compared with in vivo assessment. Toxicol. Vitr 29, 502–511. 10.1016/j.tiv.2014.12.023.

Karlsson HL, Cronholm P, Gustafsson J, Möller L, 2008. Copper oxide nanoparticles are highly toxic: a comparison between metal oxide nanoparticles and carbon nanotubes. Chem. Res. Toxicol 21, 1726–1732. 10.1021/tx800064j. [PubMed: 18710264]

Kim JS, Peters TM, O'Shaughnessy PT, Adamcakova-Dodd A, Thorne PS, 2013. Validation of an in vitro exposure system for toxicity assessment of air-delivered nanomaterials. Toxicol. Vitr 27, 164–173. 10.1016/j.tiv.2012.08.030.

Kooter IM, Gröllers-Mulderij M, Steenhof M, Duistermaat E, van Acker FAA, Staal YCM, Tromp PC, Schoen E, Kuper CF, van Someren E, 2016. Cellular effects in an In Vitro human 3D cellular airway model and A549/BEAS-2B In Vitro Cell cultures following air exposure to cerium oxide particles at an air-liquid interface. Appl. Vitr. Toxicol 2, 56–66. 10.1089/aivt.2015.0030.

Kooter IM, Gröllers-Mulderij M, Duistermaat E, Kuper F, Schoen ED, 2017. Factors of concern in a human 3D cellular airway model exposed to aerosols of nanoparticles. Toxicol. Vitr 44, 339–348. 10.1016/j.tiv.2017.07.006.

Kroll A, Pillukat MH, Hahn D, Schnekenburger J, 2009. Current in vitro methods in nanoparticle risk assessment: limitations and challenges. Eur. J. Pharm. Biopharm 72, 370–377. 10.1016/j.ejpb.2008.08.009. [PubMed: 18775492]

Kroll A, Pillukat MH, Hahn D, Schnekenburger J, 2012. Interference of engineered nanoparticles with in vitro toxicity assays. Arch. Toxicol 86, 1123–1136. 10.1007/s00204-012-0837-z. [PubMed: 22407301]

Lednicky J, Pan M, Loeb J, Hsieh H, Eiguren A, Hering S, Fan ZH, Wu C, 2016. Highly efficient collection of infectious pandemic influenza H1N1 virus (2009) through laminar-flow water based condensation. Aerosol Sci. Technol 50, 1–4. 10.1080/02786826.2016.1179254.

Leibrock L, Wagener S, Singh AV, Laux P, Luch A, 2019. Nanoparticle induced barrier function assessment at liquid-liquid and air-liquid interface in novel human lung epithelia cell lines. Toxicol. Res 1016–1027. 10.1039/c9tx00179d.

Lenz AG, Karg E, Brendel E, Hinze-Heyn H, Maier KL, Eickelberg O, Stoeger T, Schmid O, 2013. Inflammatory and oxidative stress responses of an alveolar epithelial cell line to airborne zinc oxide nanoparticles at the air-liquid interface: a comparison with conventional, submerged cell-culture conditions. Biomed. Res. Int 2013 10.1155/2013/652632.

Li Y, Li P, Yu H, Bian Y, 2016. Recent advances (2010–2015) in studies of cerium oxide nanoparticles' health effects. Environ. Toxicol. Pharmacol 44, 25–29. 10.1016/j.etap.2016.04.004. [PubMed: 27088851]

Lichtveld KM, Ebersviller SM, Sexton KG, Vizuete W, Jaspers I, Jeffries HE, 2012. In vitro exposures in diesel exhaust atmospheres: resuspension of PM from filters versus direct deposition of PM from air. Environ. Sci. Technol 46, 9062–9070. 10.1021/es301431s. [PubMed: 22834915]

Longest PW, Xi J, 2008. Condensational growth may contribute to the enhanced deposition of cigarette smoke particles in the upper respiratory tract. Aerosol Sci. Technol 42, 579–602. 10.1080/02786820802232964.

Mülhopt S, Dilger M, Diabaté S, Schlager C, Krebs T, Zimmermann R, Buters J, Oeder S, Wäscher T, Weiss C, Paur HR, 2016. Toxicity testing of combustion aerosols at the air-liquid interface with a self-contained and easy-to-use exposure system. J. Aerosol Sci 96, 38–55. 10.1016/j.jaerosci.2016.02.005.

May KR, 1973. The collison nebulizer: description, performance and application. J. Aerosol Sci 4 10.1016/0021-8502(73)90006-2.

Monteiller C, Tran L, MacNee W, Faux S, Jones A, Miller B, Donaldson K, 2007. The pro-inflammatory effects of low-toxicity low-solubility particles, nanoparticles and fine particles, on epithelial cells in vitro: the role of surface area. Occup. Environ. Med 64, 609–615. 10.1136/oem.2005.024802. [PubMed: 17409182]

Norhafana M, Noor MM, Hairuddin AA, Harikrishnan S, Kadirgama K, Ramasamy D, 2020. The effects of nano-additives on exhaust emissions and toxicity on mankind. Mater. Today Proc 8–12. 10.1016/j.matpr.2019.12.110.

Oldham MJ, Castro N, Zhang J, Rostami A, Lucci F, Pithawalla Y, Kuczaj AK, Gilman IG, Kosachevsky P, Hoeng J, Lee KM, 2019. Deposition efficiency and uniformity of monodisperse solid particle deposition in the Vitrocell® 24/48 Air-Liquid-Interface in vitro exposure system. Aerosol Sci. Technol 54, 52–65. 10.1080/02786826.2019.1676877.

Ong KJ, Maccormack TJ, Clark RJ, Ede JD, Ortega VA, Felix LC, Dang MKM, Ma G, Fenniri H, Veinot JGC, Goss GG, 2014. Widespread Nanoparticle-Assay Interference: implications for Nanotoxicity Testing. PLoS ONE 9. 10.1371/journal.pone.0090650.

Pan M, Hsieh H, Hering SV, Lednicky J, Hugh Z, 2016. Efficient collection of viable virus aerosol through laminar-flow, water-based condensational particle growth. Appl. Microbiol 120, 805–815. 10.1111/jam.13051.

Panas A, Comouth A, Saathoff H, Leisner T, Al-Rawi M, Simon M, Seemann G, Dössel O, Mülhopt S, Paur HR, Fritsch-Decker S, Weiss C, Diabaté S, 2014. Silica nanoparticles are less toxic to human lung cells when deposited at the air-liquid interface compared to conventional submerged exposure. Beilstein J. Nanotechnol 5, 1590–1602. 10.3762/bjnano.5.171. [PubMed: 25247141]

Park B, Donaldson K, Duffin R, Tran L, Kelly F, Mudway I, Morin JP, Guest R, Jenkinson P, Samaras Z, Giannouli M, Kouridis H, Martin P, 2008. Hazard and risk assessment of a nanoparticulate cerium oxide-based diesel fuel additive - a case study. Inhal. Toxicol 20, 547–566. 10.1080/08958370801915309. [PubMed: 18444008]

Paur H, Cassee FR, Teeguarden J, Fissan H, Diabate S, Aufderheide M, Kreyling WG, Otto H, Kasper G, Riediker M, Rothen-rutishauser B, Schmid O, 2011. In-vitro cell exposure studies for the assessment of nanoparticle toxicity in the lung — a dialog between aerosol science and biology. J. Aerosol Sci 42, 668–692. 10.1016/j.jaerosci.2011.06.005.

Rach J, Budde J, Mohle N, Aufderheide M, 2014. Direct exposure at the air-liquid interface: evaluation of an in vitro approach for simulating inhalation of airborne substances. J. Appl. Toxicol 34, 506–515. 10.1002/jat.2899. [PubMed: 23765558]

Raemy DO, Limbach LK, Rothen-Rutishauser B, Grass RN, Gehr P, Birbaum K, Brandenberger C, Günther D, Stark WJ, 2011. Cerium oxide nanoparticle uptake kinetics from the gas-phase into lung cells in vitro is transport limited. Eur. J. Pharm. Biopharm 77, 368–375. 10.1016/j.ejpb.2010.11.017. [PubMed: 21118721]

Raemy DO, Grass RN, Stark WJ, Schumacher CM, Clift MJD, Gehr P, Rothen – Rutishauser B, 2012. Effects of flame made zinc oxide particles in human lung cells - a comparison of aerosol and suspension exposures. Part. Fibre Toxicol 9, 33. 10.1186/1743-8977-9-33. [PubMed: 22901679]

Rampersad SN, 2012. Multiple applications of alamar blue as an indicator of metabolic function and cellular health in cell viability bioassays. Sensors 12, 12347–12360. 10.3390/s120912347. [PubMed: 23112716]

Ren ZX, Bin Yu H, Li JS, Shen JL, Sen Du W, 2015. Suitable parameter choice on quantitative morphology of A549 cell in epithelial-mesenchymal transition. Biosci. Rep 35, 1–7. 10.1042/BSR20150070.

Ristovski ZD, Miljevic B, Surawski NC, Morawska L, Fong KM, Goh F, Yang IA, 2012. Respiratory health effects of diesel particulate matter. Respirology 17, 201–212. 10.1111/j.1440-1843.2011.02109.x. [PubMed: 22126432]

Saxena V, Kumar N, Kumar VK, 2017. A comprehensive review on combustion and stability aspects of metal nanoparticles and its additive effect on diesel and biodiesel fuelled C.I. engine, Renew. Sustain. Energy Rev 70, 563–588. 10.1016/j.rser.2016.11.067.

Schneider CA, Rasband WS, Eliceiri KW, 2012. NIH Image to ImageJ: 25 years of image analysis. Nat. Methods 9, 671–675. 10.1038/nmeth.2089. [PubMed: 22930834]

Setiabudi A, Chen J, Mul G, Makkee M, Moulijn JA, 2004. CeO_2 catalysed soot oxidation: the role of active oxygen to accelerate the oxidation conversion. Appl. Catal. B Environ 51, 9–19. 10.1016/j.apcatb.2004.01.005.

Snow SJ, Mcgee J, Miller DB, Bass V, Schladweiler MC, Thomas RF, Krantz T, King C, Ledbetter AD, Richards J, Weinstein JP, Conner T, Willis R, Linak WP, Nash D, Wood CE, Elmore SA, Morrison JP, Johnson CL, Gilmour MI, Kodavanti UP, 2014. Inhaled diesel emissions generated with cerium oxide nanoparticle fuel additive induce adverse pulmonary and systemic effects. Toxicol. Sci 142, 403–417. 10.1093/toxsci/kfu187. [PubMed: 25239632]

Stewart CE, Torr EE, Mohd Jamili NH, Bosquillon C, Sayers I, 2012. Evaluation of differentiated human bronchial epithelial cell culture systems for asthma research. J. Allergy 2012, 1–11. 10.1155/2012/943982.

Stone V, Johnston H, Schins RPF, 2009. Development of in vitro systems for nanotoxicology: methodological considerations in vitro methods for nanotoxicology. Crit. Rev. Toxicol 39, 613–626. 10.1080/10408440903120975. [PubMed: 19650720]

Teeguarden JG, Hinderliter PM, Orr G, Thrall BD, Pounds JG, 2007. Particokinetics in vitro: dosimetry considerations for in vitro nanoparticle toxicity assessments. Toxicol. Sci 95, 300–312. 10.1093/toxsci/kfl165. [PubMed: 17098817]

Tilly TB, Kerr LL, Braydich-Stolle LK, Schlager JJ, Hussain SM, 2014. Dispersions of geometric TiO_2 nanomaterials and their toxicity to RPMI 2650 nasal epithelial cells. J. Nanoparticle Res 16, 2695. 10.1007/s11051-014-2695-5.

Tilly TB, Ward RX, Luthra JK, Robinson SE, Eiguren-Fernandez A, Lewis GS, Salisbury RL, Lednicky JA, Sabo-Attwood TL, Hussain SM, Wu CY, 2019. Condensational particle growth device for reliable cell exposure at the air-liquid interface to nanoparticles. Aerosol Sci. Technol 53, 1415–1428. 10.1080/02786826.2019.1659938. [PubMed: 33033421]

Tilly TB, Nelson MT, Chakravarthy KB, Shira EA, Debrose MC, Grabinski CM, Salisbury RL, Mattie DR, Hussain SM, 2020. In Vitro aerosol exposure to nanomaterials: from laboratory to environmental field toxicity testing. Chem. Res. Toxicol 10.1021/acs.chemrestox.9b00237.

Ward RX, Tilly TB, Mazhar SI, Robinson SE, Eiguren-Fernandez A, Wang J, Sabo-Attwood T, Wu CY, 2020. Mimicking the human respiratory system: online in vitro cell exposure for toxicity assessment of welding fume aerosol. J. Hazard. Mater 395, 122687 10.1016/j.jhazmat.2020.122687.

Wu CY, Biswas P, 2005. Nanoparticles and the environment. J. Air Waste Manag. Assoc 55, 708–746. 10.1080/10473289.2005.10464656. [PubMed: 16022411]

Wu J, Wang Y, Liu G, Jia Y, Yang J, Shi J, Dong J, Wei J, Liu X, 2018. Characterization of air-liquid interface culture of A549 alveolar epithelial cells. Brazilian J. Med. Biol. Res 51, 1–9. 10.1590/1414-431x20176950.

Zavala J, Greenan R, Krantz QT, DeMarini DM, Higuchi M, Gilmour MI, White PA, 2017. Regulating temperature and relative humidity in air-liquid interface in vitro systems eliminates cytotoxicity resulting from control air exposures. Toxicol. Res 6, 448. 10.1039/C7TX00109F.

Zhang J, Nazarenko Y, Zhang L, Calderon L, Lee KB, Garfunkel E, Schwander S, Tetley TD, Chung KF, Porter AE, Ryan M, Kipen H, Lioy PJ, Mainelis G, 2013. Impacts of a nanosized ceria additive on diesel engine emissions of particulate and gaseous pollutants. Environ. Sci. Technol 47, 13077–13085. 10.1021/es402140u. [PubMed: 24144266]

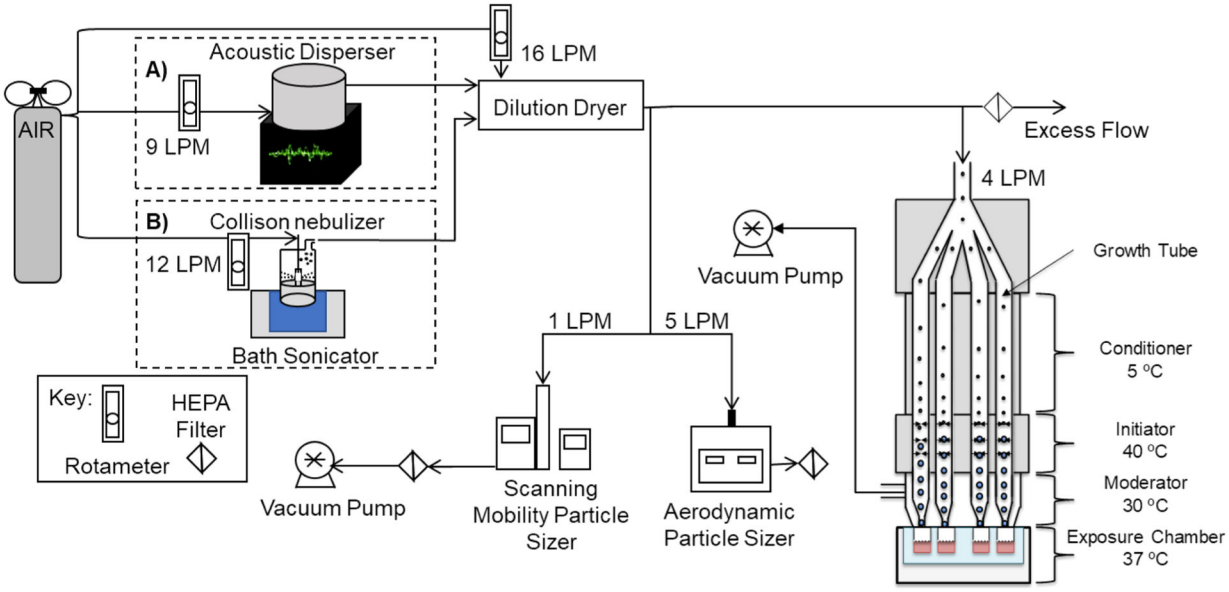

Fig. 1.

Schematic for nanoparticle aerosolization, particle size measurement, and ALI cell exposure in DAVID.

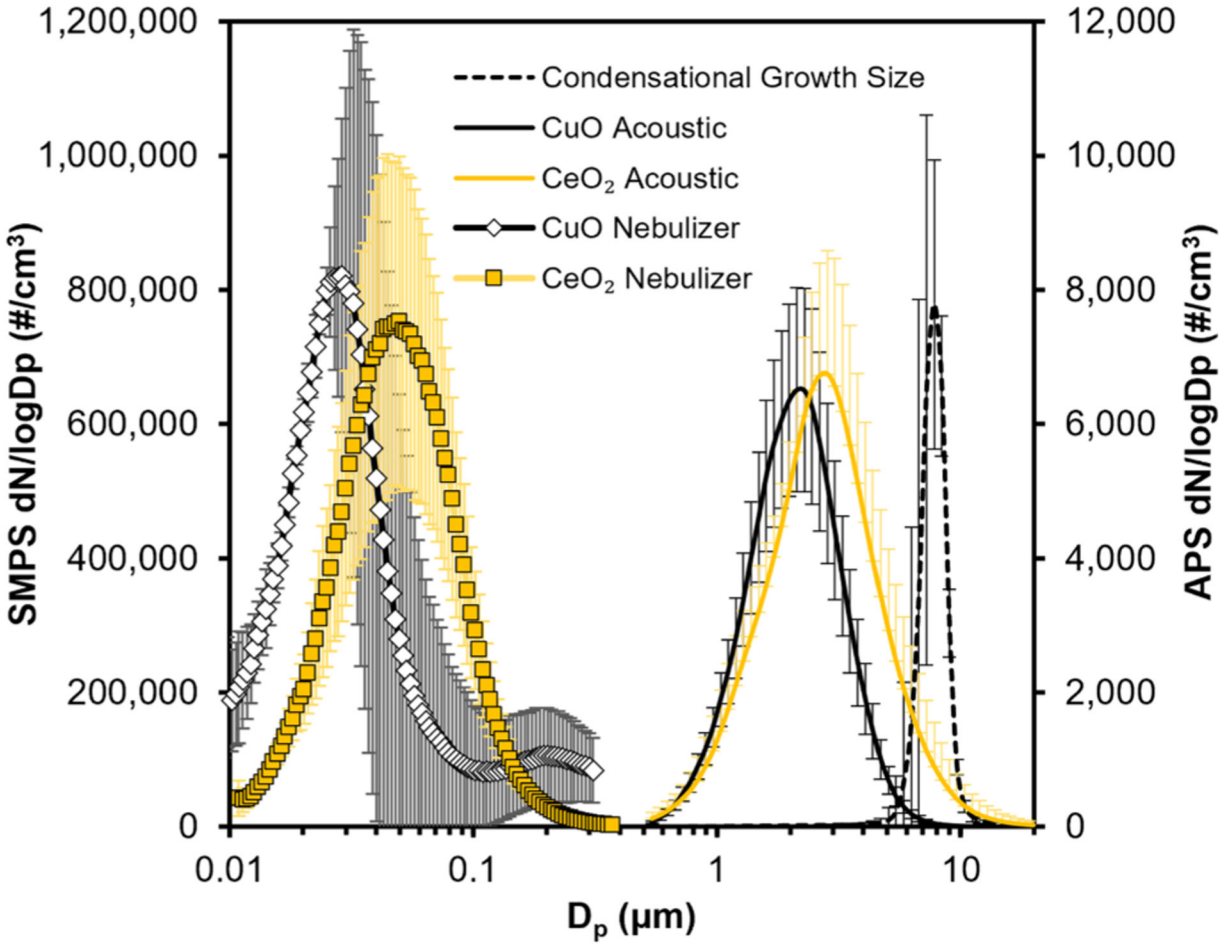

Fig. 2.

Particle size measurements by SMPS (left side) and APS (right side) of the CeO_2 and CuO nanoparticle aerosols generated by nebulizer and acoustics, and final condensational particle growth droplet diameter of all the aerosols.

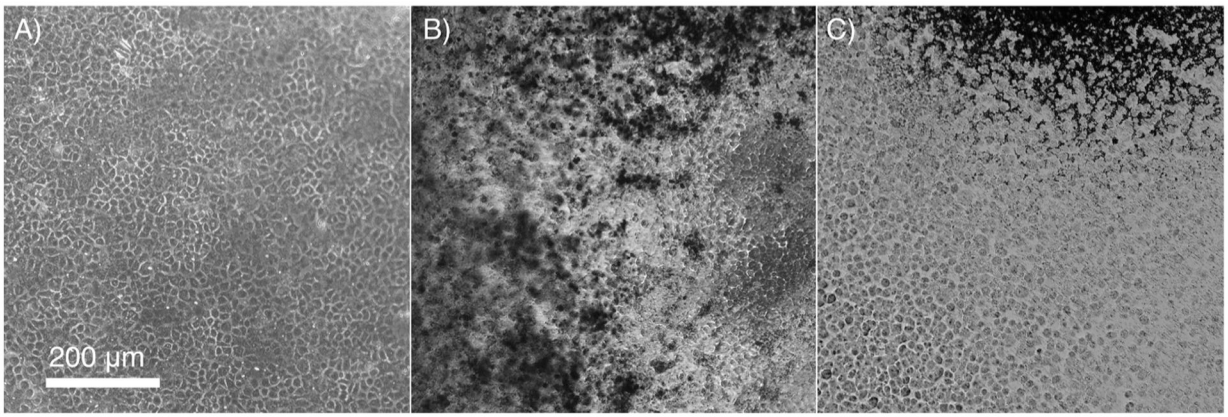

Fig. 3.

Light microscopy images of A) ALI cell culture, B) ALI exposure to CeO_2 NPs, and C) ALI exposure to CuO NPs. With 10x objective and 10x ocular.

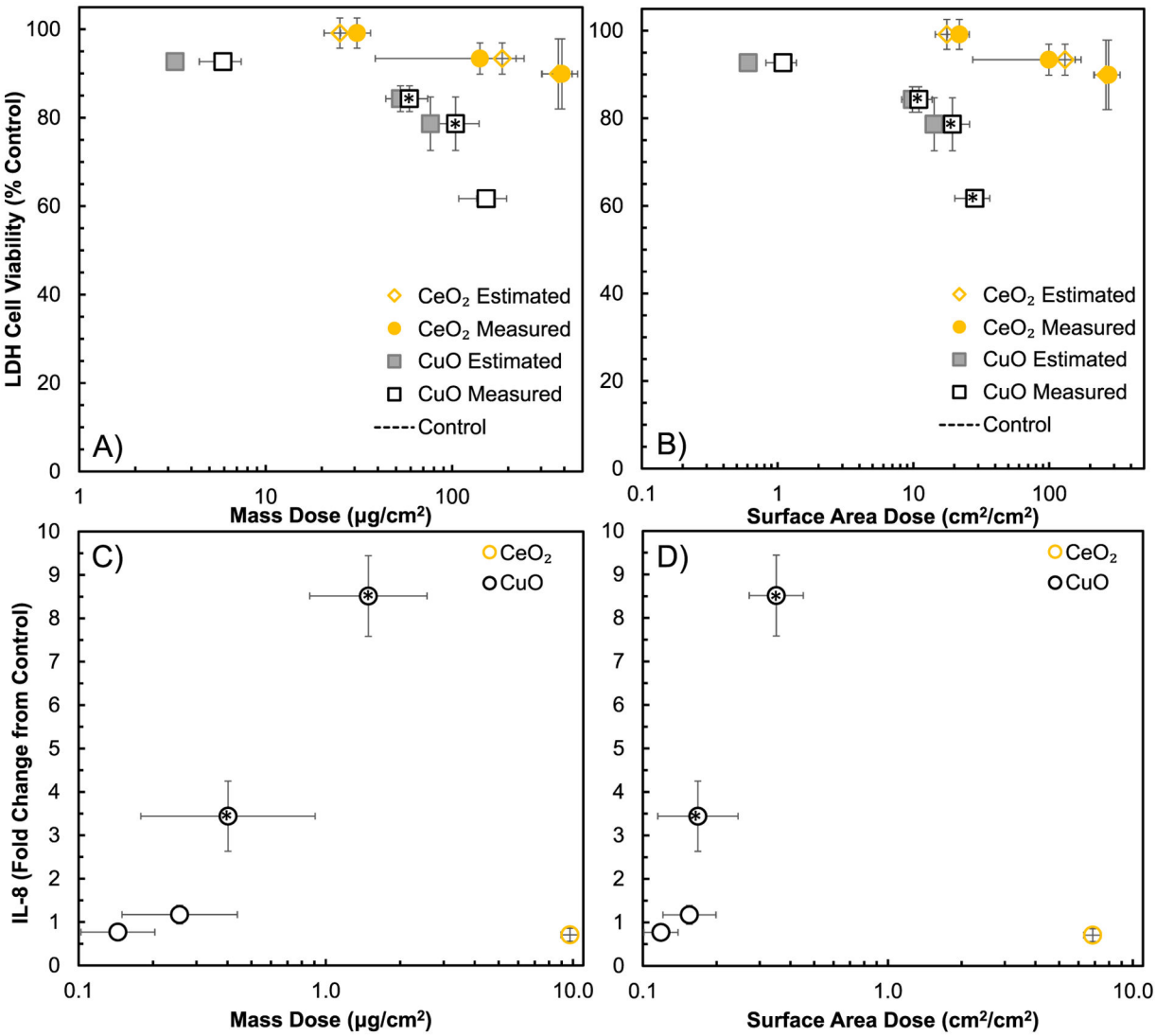

Fig. 4.

Global dose response of ALI cell cultures exposed to CeO_2 and CuO NPs. The LDH cell viability for A549 cells exposed to a delivered NP dose estimated from aerosol data and measured by ICP-MS in A) mass and B) surface area. The IL-8 cytokine fold change from clean air exposure control based on C) mass dose and D) surface area dose. Logscale is used on the horizontal axis to compare the doses more easily with the assay endpoints, and statistical significance (α=0.05) from the control is indicated by (*).

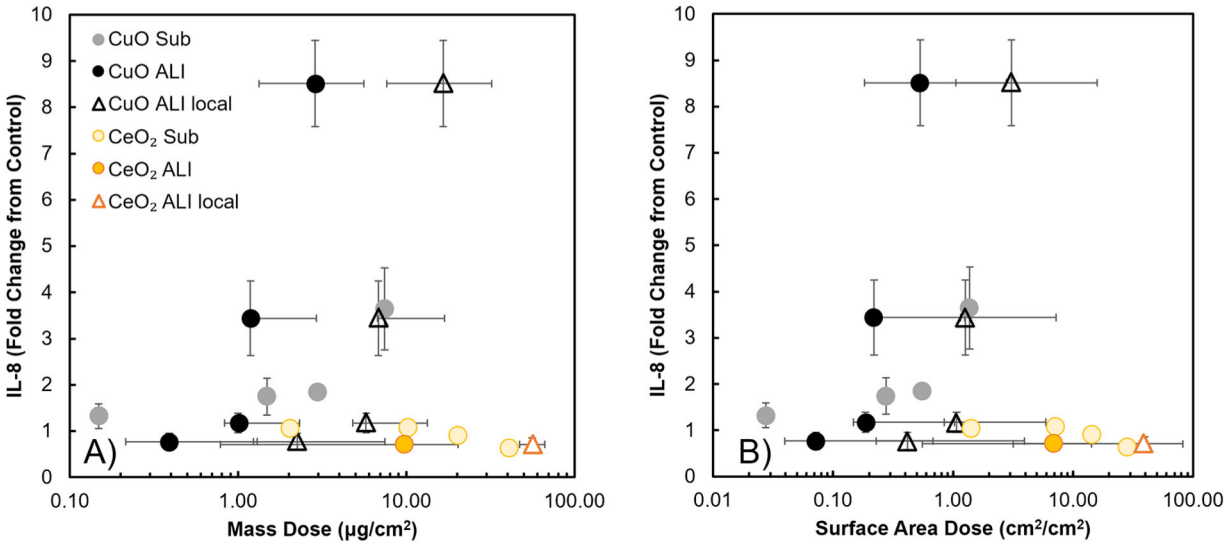

Fig. 5.

IL-8 cytokine excretion (fold change from control) for the submerged and ALI cell exposures to CuO and CeO_2 NPs, shown in log scale, for the A) mass dose and B) surface area dose. ALI results are presented in both global (averaged across the cell culture) and local (at the NP deposition spot) doses.